The deformation field of the August 2003 eruption at Piton de la Fournaise, Reunion Island, mapped by ASAR interferometry

J.-L. Froger,[1] Y. Fukushima,[2] P. Briole,[3] T. Staudacher,[4] T. Souriot,[2] and N. Villeneuve[5]

Received 8 May 2004; revised 11 June 2004; accepted 17 June 2004; published 16 July 2004.

[1] Three independent ASAR interferograms spanning the August 2003 Piton de la Fournaise eruption, reveal a 3 by 3 km asymmetric pattern of range changes centred on the Dolomieu crater northern flank. It corresponds to 30 cm of displacement towards the satellite east of the eruptive fissures and 7 cm away from the satellite west of the fissures. Displacements are caused by dyke emplacement below fissures. We model the deformation using a 3D mixed boundary element method for elastic media. This consists of a dyke defined by six geometric parameters and an overpressure gradient. A neighbourhood algorithm was applied to explore this 7 dimensional parameter space. The best-fit model is a 57° eastward dipping dyke with a base lying around 1520 m a.s.l. The model provides new evidence of the dyke intrusion – related seaward displacements of the volcano eastern flank. *INDEX TERMS:* 0933 Exploration Geophysics: Remote sensing; 1244 Geodesy and Gravity: Standards and absolute measurements; 3210 Mathematical Geophysics: Modeling; 6924 Radio Science: Interferometry; 8419 Volcanology: Eruption monitoring (7280).
Citation: Froger, J.-L., Y. Fukushima, P. Briole, T. Staudacher, T. Souriot, and N. Villeneuve (2004), The deformation field of the August 2003 eruption at Piton de la Fournaise, Reunion Island, mapped by ASAR interferometry, *Geophys. Res. Lett.*, *31*, L14601, doi:10.1029/2004GL020479.

1. Introduction

[2] Piton de la Fournaise volcano forms the SE part of La Réunion, an oceanic basaltic island in the southernmost part of Mascarene Basin (Indian Ocean) (Figure 1). More than 150 eruptions, producing mostly fluid basaltic lava flows within Enclos Fouqué caldera, have been documented since the 17th century. Eruptive fissures and vents are roughly clustered along two fracture zones trending N10°E and S10°E [*Lénat and Bachèlery*, 1990]. At the intersection of these two fracture zones, the central cone, 400 m high and 3 km wide, has an elongated east-west shape. There are two summit pit-craters, Bory and Dolomieu (Figure 1).

[3] From 12 July 2003, seismic activity at Piton de la Fournaise increased. Focal depth of the strongest events were clustered at about 1 km above sea level, below Bory crater. At the same time, the GPS measurements made by the Piton de la Fournaise Volcano Observatory (OVPF) show a volcano-wide inflation, reaching 30 cm in the central area. On August 23, at about 2120 UT, a first fissure opened in Bory crater [*Staudacher*, 2003]. A second fissure opened at 2210 UT on the north flank at 2460 m. Both fissures remained active for a short time. At 2330 UT a final fissure opened on the north flank below the second fissure, at 2200 m. Subsequent activity focused here, forming the Piton Payenkë cinder cone from which lava flow moved down into La Plaine des Osmondes. The 36 hours following the initial activity were characterized by a substantial increase in tremor intensity and lava emission, but at 2158 UT on 27 August the eruption abruptly ceased. The volume of lava emitted during this time is estimated to 5.6×10^6 m^3.

2. InSAR Measurements by ASAR

[4] We present a preliminary analysis of the displacements related to the August 2003 eruption, using the Synthetic Aperture Radar Interferometry (INSAR) technique with images acquired by the Advanced Synthetic Aperture Radar (ASAR). The INSAR technique calculates the difference in phase, i.e., the interferogram, between two images acquired for the same area at different epochs by radar satellites. As displacements modify the distance between ground and satellite (thus changing the radar wave propagation time) they result in phase changes expressed as fringe patterns in the interferogram [*Massonnet and Feigl*, 1998]. INSAR has been successfully used since 1995 to monitor surface displacement related to volcanic activity, with data provided by the European ERS-1 and ERS-2 satellites, the Japanese JERS-1 satellite and the Canadian RADARSAT-1 satellite [*Massonnet and Feigl*, 1998; *Stevens and Wadge*, 2004]. However, very little work has been done so far on Piton de la Fournaise using this technique. The main reason is that no ERS and very few JERS data have been acquired for Reunion Island. Up to now, the main source of INSAR data was the commercial RADARSAT-1 satellite. *Sigmundsson et al.* [1999] used these data to map the displacements caused by the March–September 1998 eruption. Their interferograms show up to seventeen fringes, indicating a ground displacement towards the satellite of almost 50 cm. They calculated the theoretical change in range using an Okada formulation for dislocations [*Okada*, 1985] which assumes that rectangular fractures, located in an elastic half space, undergo constant displacements. A detailed analysis was also done by

[1]Institut de Recherche pour le Développement (IRD) UR31 "Processus et Aléas Volcaniques", LMV, UBP-UMR 6524, Clermont-Ferrand, France.
[2]Laboratoire Magmas et Volcans, Université Blaise Pascal-UMR 6524, Clermont-Ferrand, France.
[3]Institut de Physique du Globe de Paris, CNRS-UMR 7580, Paris, France.
[4]Observatoire Volcanologique du Piton de la Fournaise, Institut de Physique du Globe de Paris, La Plaine des Cafres, La Reunion.
[5]Centre de recherches et d'études en géographie de l'Université de La Réunion (CREGUR), Université de la Réunion, Saint-Denis, La Reunion.

0094-8276/04/2004GL020479$05.00

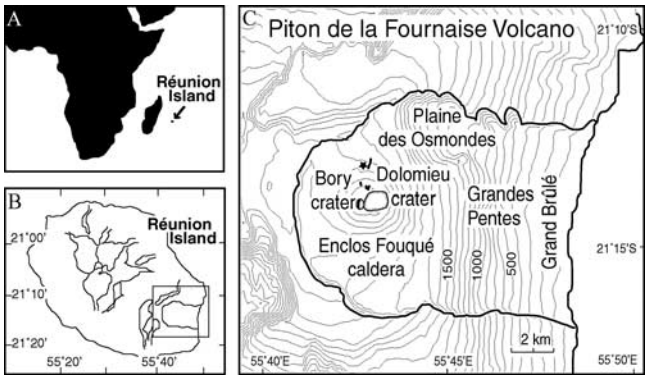

Figure 1. a) Location of Réunion Island in the Indian Ocean; b) Location of Piton de la Fournaise volcano; c) Topography of Piton de la Fournaise with 100 m elevation contours and location of the main places discussed in text. The location of the August 2003 eruptive fissures is indicated in black. The star is the location of Piton Payenké.

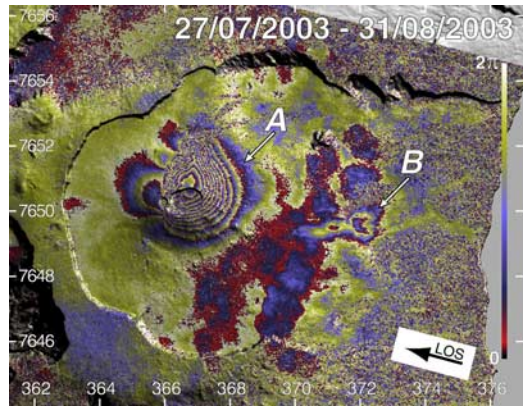

Figure 2. Interferogram spanning 35 days from 27 July to 8 August 2003. The phases have been draped on the shaded DEM. A complete cycle of phase (red-blue-yellow) represents an increase in range of 2.8 cm between the ground surface and the satellite. a) fringe pattern related to the August 2003 eruption; b) fringe pattern related to the compaction of recent lava flows. Coordinates in kilometers UTM (40 zone South).

Fukushima et al. [2003] from RADARSAT-1 data for the February 2000 eruption. They used a 3D mixed boundary element method (3-D MBEM) for elastic medium that allows to obtain a more realistic model than a simple Okada approach.

[5] Launched in March 2002 by the European Space Agency (ESA), ENVISAT is dedicated to Earth observation. Its payload includes a radar, ASAR, designed to continue the observations began with the SAR onboard the ERS satellites. It operates in the C-band (5.331 GHz), repeats its track every 35 days and can image seven different swaths with incidence angles from 15 to 45 degrees. By acquiring all swaths both in ascending and descending pass it is theoretically possible to image the same ground target with a mean repetition cycle of 2.5 days; although only the images acquired under the same track and the same swath can be combined to produce an interferogram. An important improvement of ENVISAT, with respect to ERS satellites, is the high capability of the onboard data recorders and the possibility to relay the data to Earth via the ESA Artemis satellite. Hence ENVISAT is able to image almost every place in the world without having to be directly in contact with a ground station (the reason for which no ERS data were acquired on Reunion Island).

3. Data

[6] We have used six Single Look Complex images produced by ESA from raw data collected between July and September by the ASAR instrument (Table 1). From this dataset, we computed three interferograms using the Diapason software [*Centre National d'Etudes Spatiales*, 1996]. The contribution of the orbital trajectories was modeled and removed using the orbit state vectors delivered with the image file. We modeled and removed the topography with a 25 × 25 m Digital Elevation Model (DEM) made by the French Geographic Institute (IGN). The DEM was also used to georeference the interferograms.

[7] The interferograms exhibit a good coherence in areas covered by barren lava flows (mostly inside the Enclos Fouqué caldera) (Figure 2). Outside the caldera and in the Grand Brulé the coherence is poor because of vegetation. Due to its very low altitude of ambiguity (h_a, Table 1), the ascending interferogram is significantly less coherent than the two descending ones. The ascending interferogram also has strong geometric distortions (foreshortening and layover), similar to those generally observed in ERS interferograms. In fact, the ASAR swath 2 acquisition mode is the closest to the ERS acquisition characteristics. In contrast, due to the relatively high incidence angles of swathes 6 and 7, the foreshortening and layover are small on the descending interferograms.

[8] The most prominent feature of the interferograms is a concentric fringe pattern on the central cone. The pattern is very similar on both descending interferograms. It is

Table 1. Parameters of the Three Interferograms

	Interferogram 1	Interferogram 2	Interferogram 3
Pass	Ascending	Descending	Descending
Swath/Track	2/313	6/277	7/005
Incidence angle[a]	23°	41°	44°
Unit Vector [East, North, Up][b]	[−0.38, −0.08, 0.92]	[0.64, −0.15, 0.75]	[0.68, −0.15, 0.72]
Date 1	29/07/2003	27/07/2003	12/08/2003
Date 2	02/09/2003	31/08/2003	16/09/2003
h_a[c] (m)	15	1037	−39

[a]From the vertical.
[b]From ground to satellite at midswath for the Piton de la Fournaise latitude.
[c]The altitude of ambiguity h_a gives an estimate of the sensibility of the interferogram to the topography.

significantly different in shape and amplitude on the ascending interferogram, and not very well defined because of the strong foreshortening on the western flank of the central cone.

[9] As the three interferograms have very different h_a (Table 1) and were produced from images acquired on different days, the fringe pattern could be attributed only to ground deformations between the 12–31 August 2003. On the descending interferograms, the fringe pattern is asymmetric with respect to the eruptive fissures, as it was already observed in the case of the 1998 eruption [*Sigmundsson et al.*, 1999]. On the unbuttressed east side, up to eleven fringes are visible on the descending interferograms and about four fringes are seen on the ascending interferogram. They indicate a range decrease between the ground and the satellite of about 30 cm and 11 cm respectively. The difference in the magnitude of range changes between the descending and the ascending interferograms is an evidence that a significant part of the displacements is horizontal. Only one and half fringes are visible on the buttressed western side of the volcano indicating a range increase of about 4 cm. The maximum displacement appears 500 m east of the eruptive fissure, north of the Dolomieu pit-crater. All these observations are compatible with the opening of an eastward-dipping dyke.

[10] A second, more subtle, fringe pattern is visible in the area of the Grandes Pentes (Figure 2). It coincides with recent lava flows (Marsh 2001, June, July and November 2002). It most likely corresponds to ongoing thermomechanical compaction.

4. Modeling

[11] In order to characterize the source of the deformation, we have modeled the displacements using 3-D MBEM, considering a uniform elastic half-space [*Cayol and Cornet*, 1998]. The 3-D MBEM can incorporate realistic topography and geometrical complexities of deformation sources such as fractures or magma reservoirs. In our case, a 3-D method is particularly necessary as the displacements occur on significant topography. We produced a mesh of the ground surface from the IGN DEM. It is made of triangular elements with size gradually increasing from 1.6×10^3 m^2 near the eruptive fissures to 5.6×10^5 m^2 near the edge of the mesh. The modelled displacements and the residues are calculated at the nodes of this mesh. The source of the deformation is modelled by a dyke defined by 6 geometric parameters: the mean dyke dip, the mean bottom side elevation, the bottom side inclination, the angle between the top and the bottom sides (twist), the inclination of the vertical side (shear), and the length ratio between the top and the bottom sides. A seventh parameter is the dyke magma over-pressure gradient. In order to find the best fit model, we explored the 7-D parameter space using a neighbourhood algorithm [*Sambridge*, 1999]. This search method is based on dividing the multidimensional parameter space into convex polyhedra (Voronoi cells), each of them being centred on a set of parameters with misfit values. We define the misfit function as the normalized root-mean square-error between the observed and calculated displacements. The observed displacements are obtained from interferograms by unwrapping the phases, using an iterative procedure based on the Snaphu software [*Chen and Zebker*, 2002]. The calculated displacements are obtained by computing the dot product $\boldsymbol{s} \cdot \boldsymbol{u}$ where $\mathbf{s}$ is the three-dimensional displacement resulting from the 3-D MBEM calculation and $\mathbf{u}$ the unit vector from ground to satellite. At each iteration n_s new samples are put into n_r Voronoi cells which are chosen after evaluating the misfit values. The best model is that which minimizes the misfit function.

Table 2. Summary of the Results of Inversions[1]

	Inversion 1	Inversion 2
Asc. Interferogram	29/07/03 – 02/09/03	29/07/03 – 02/09/03
Desc. Interferogram	27/07/03 – 31/08/03	12/08/03 – 16/09/03
Results[a]		
Number of calculations	5800	6450
Dip (°)	59.32 ± 3.89	53.13 ± 2.43
Shear (°)	−26.11 ± 11.54	−29.32 ± 8.69
Bottom Elevation (m)	1461.85 ± 169.76	1583.47 ± 55.73
BotLenRate[b] (%)	0.88 ± 0.17	0.72 ± 0.10
Twist (°)	10.54 ± 7.43	21.61 ± 4.16
Bottom Inclination (°)	3.89 ± 9.00	3.29 ± 3.70
Pgrad (MPa/m)[c]	1.0×10^{-3}	3.0×10^{-3}
P_0 (MPa)[d]	0.45	0.89
Average opening (m)	0.29	0.31
Dyke volume (m^3)	8.1×10^5	7.4×10^5
Misfit (%)[e]	10.99	12.88

[a]The values of the best-fit parameters are reported ± two standard deviations.
[b]Top length/bottom length ratio.
[c]Magma overpressure gradient in the dyke.
[d]Magma overpressure at the bottom of the dyke.
[e](100 − Misfit) gives the percentage of explained data.

[12] Two independent inversions were performed. In the first, we have jointly inverted the interferograms 1 and 2 and in the second one, the interferograms 1 and 3. The incidence angles of swathes 6 and 7 are very close, so that interferograms 2 and 3 provide similar constraints on the displacement components. Independent inversions on these allowed us to check the method consistency. We used broad bounds on the parameter values, since we had little a priori constraints on the deformation source. We obtained two best fit models that explain 89 % and 87 % respectively of the observed data (Table 2). The parameters of each are close, indicating that the observations could be explained by a dyke with a dip around 56° to the east and whose bottom lies around 1500 m a.s.l., below the Dolomieu crater. The length of the modeled dyke is 12% to 28% shorter at its base than at its top. This is consistent with the geometry observed for artificial hydraulic fractures. The corresponding average opening is 30 cm, with an overpressure between 0.45 and 0.89 MPa at the base of the dyke and an overpressure gradient between 1.0 and 3.0 KPa/m.

[13] The models could be considered satisfactory in reproducing the larger wavelengths of the observed deformation pattern (Figure 3). They are also in good agreement with the displacement vectors obtained from GPS measurements by the OVPF during the August eruption.

5. Discussion and Conclusions

[14] The calculated range of the dip value (53°–60° eastward) and the strike of the August 2003 dyke are

[1]Auxiliary material is available at ftp://ftp.agu.org/apend/gl/2004GL020479.

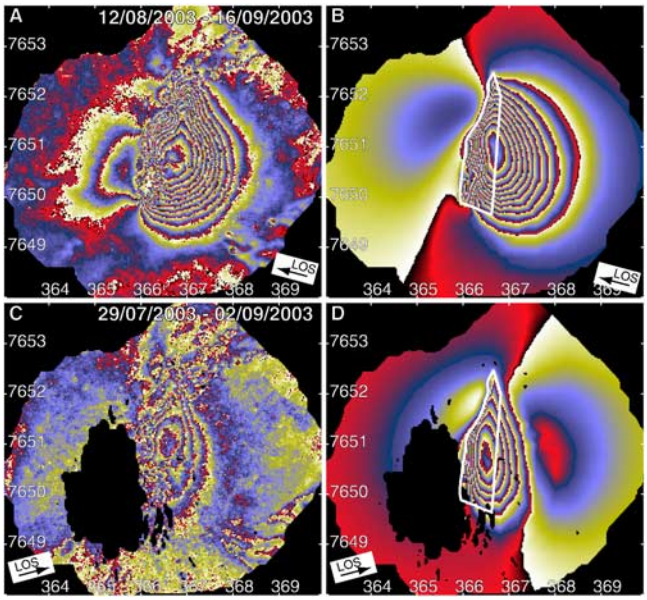

Figure 3. a) Descending interferogram spanning 35 days from 12 August to 16 September 2003; b) modeled interferogram obtained by projecting the best fit model (inversion 2) deformation map in the geometry of interferogram displayed in A; White contour indicates the surface projection of the modeled dyke; c) Ascending interferogram spanning 35 days from 29 July to 2 September 2003; D) modeled interferogram obtained by projecting the best fit model (inversion 2) deformation map in the geometry of interferogram displayed in C; Coordinates in kilometers UTM (40 zone South).

close to those proposed by *Battaglia and Bachèlery* [2003] for the March 1998 eruption (53°–58° eastward) and those proposed by *Fukushima et al.* [2003] for the February 2000 eruption (59° eastward). Our values for the dyke dip and its basal depth suggest an origin close, although slightly shifted eastward, to the cluster of pre-eruption seismic events. This is similar to the interpretation of the March 1998 intrusion by *Battaglia and Bachèlery* [2003]. Also, the displacement patterns imaged by RADARSAT-1 data for the March 1998 [*Sigmundsson et al.*, 1999] and February 2000 [*Fukushima et al.*, 2003] eruptions and by ASAR for the August 2003 eruption are remarkably similar. This indicates that significant seaward displacement of the eastern flank of Piton de la Fournaise occurred during each intrusion. All these observations suggest a general mechanical behaviour of the edifice in response to the intrusions. As previously proposed by *Sigmundsson et al.* [1999], we stress that repeated dyke injections within the Enclos Fouqué, along the general NS rift system, progressively push the eastern (seaward) flank and increase its slope, leading to a reduction of its gravitational stability. On a short time scale, this may change the regional stress field, reinforcing, by positive feedback, the probability of dyke injection in the preferential NS direction. On a longer time scale, stability could be reduced enough to trigger large flank collapses. Such events are known to have occurred recurrently in the past [*Labazuy*, 1996].

[15] The work presented here is based on only 6 ASAR images acquired during a short time span. They can only provide a discontinuous and incomplete view of the succession of events which culminated in the 22 August 2003 eruption. We have made the implicit assumption all displacement is due to dyke propagation and eruptive fissure opening, on 22 August. However, it is possible that the interferometric data integrate displacements related to the infilling then emptying of the reservoir feeding the dyke. To discriminate these different effects, it will be necessary to use both real time geodetic measurements available at OVPF (tiltmeters and GPS) and a more exhaustive INSAR database spanning the months before and after the eruption.

[16] While the modeled displacements are in good general agreement with the observations, they miss some shorter wavelength features, particularly to the west of the eruptive fissures. This is probably because we modeled the dyke as a simple quadrangular structure surfacing as a unique continuous crack. In reality, it probably has a more complex shape. In particular, it did divide, near the surface, to en-echelon eruptive fissures. More work is required to take into account these geometric complexities, without increasing critically the number of parameters to be inverted.

[17] Beyond the scope of understanding the dynamics of Piton de la Fournaise, our study demonstrates the high potentiality of ASAR-ENVISAT as a successor of ERS-1 and -2 in interferometry. The capability of the ASAR-ENVISAT system to acquire data under various angles of view is especially interesting for volcano monitoring. Volcanic provinces are generally areas with high topographic relief where geometric distortions (foreshortening – layover) of radar images can be critical. The use of data acquired with a low view angle (swathes 4–7) significantly reduces this effect, minimising information loss. This is illustrated by our data, where the ascending interferogram, calculated with images acquired in swath 2 (≈23°), has a large zone of lost information on the central cone western flank, while in the descending interferograms, calculated with images acquired in swathes 6 (≈41°) and 7 (≈44°), the loss of information is restricted to the steepest slopes (i.e., the rims of the Dolomieu and Bory craters). In addition, the possibility to image ground deformation under various angles of view is also extremely useful to improve the deformation vector accuracy (at least for the vertical and east-west components). Finally, the multiple modes of acquisition of ASAR also allow increased data acquisition (14 per 35 days), which is important for efficient volcano monitoring.

[18] On the other hand, because of the multiple modes of acquisition, making the large homogeneous temporal series needed for continuous monitoring will be a real challenge. If it is relatively easy to do so at Piton de la Fournaise, which is an isolated target, it will be much more complex for continental targets, as the probability of incompatibility is high between the various modes of acquisition required by users for targets located along the same track.

[19] **Acknowledgments.** The ASAR data were provided by European Space Agency through the EO-746 project. This work was supported by the Groupe De Recherche 515 STRAINSAR (CNRS, France). The authors would like to especially thank Jean-François Lénat, Valérie Cayol, Philippe Durand, Benjamin and Fran van Wyk de Vries for their helpful comments. The suggestions of two anonymous reviewers help us to further improve the manuscript.

References

Battaglia, J., and P. Bachèlery (2003), Dynamic dyke propagation deduced from tilt variations preceding the March 9, 1998, eruption of the Piton de la Fournaise volcano, *J. Volcanol. Geotherm. Res.*, *120*, 289–310.

Cayol, V., and F. H. Cornet (1998), Three-dimensional modelling of the 1983–1984 eruption at Piton de la Fournaise volcano, Réunion Island, *J. Geophys. Res.*, *103*, 18,025–18,037.

Centre National d'Etudes Spatiales (1996), Philosophie de mode d'emploie de la chaîne logicielle interférométrique DIAPASON, Toulouse, France.

Chen, C. W., and H. A. Zebker (2002), Phase unwrapping for large SAR interferograms: Statistical segmentation and generalized network models, *IEEE Trans. Geosci. Remote Sens.*, *40*, 1709–1719.

Fukushima, Y., P. Durand, and V. Cayol (2003), Seaward displacements at Piton de la Fournaise measured by RADAR interferometry between 1998 and 2000, paper presented at EGS-AGU-EUG Joint Assembly, Nice, France, 6–11 April .

Labazuy, P. (1996), Recurrent landslides events on the submarine flank of Piton de la Fournaise volcano (Réunion Island), in *Volcano Instability on the Earth and Other Planets*, edited by W. McGuire, A. P. Jones, and J. Neuberg, *Geol. Soc. Spec. Publ.*, *110*, 293–305.

Lénat, J.-F., and P. Bachèlery (1990), Structure and dynamics of the central zone of Piton de la Fournaise volcano, in *Le Volcanisme de la Réunion–Monographie*, edited by J.-F. Lénat, pp. 257–296, Cent. de Rech. Volcanol., Clermont-Ferrand, France.

Massonnet, D., and K. L. Feigl (1998), Radar interferometry and its application to changes in the Earth's surface, *Rev. Geophys.*, *36*, 441–500.

Okada, Y. (1985), Surface deformation due to shear and tensile faults in a half-space, *Bull. Seismol. Soc. Am.*, *75*, 1135–1154.

Sambridge, M. (1999), Geophysical inversion with a neighbourhood algorithm - I. Searching a parameter space, *Geophys. J. Int.*, *138*, 479–494.

Sigmundsson, F., P. Durand, and D. Massonnet (1999), Opening of an eruptive fissure and seaward displacement at Piton de la Fournaise volcano measured by RADARSAT satellite radar interferometry, *Geophys. Res. Lett.*, *26*, 533–536.

Staudacher, T. (2003), Volcanic activity reports, *Bull. Global Volcanism Network*, *28*, 2 pp.

Stevens, N. F., and G. Wadge (2004), Towards operational repeat-pass SAR interferometry at active volcanoes, *Nat. Hazards*, in press.

P. Briole, Institut de Physique du Globe de Paris, CNRS-UMR 7580, 4 Place Jussieu, F-75005 Paris, France.

J.-L. Froger, Institut de Recherche pour le Développement (IRD) UR31 "Processus et Aléas Volcaniques", LMV, UBP-UMR 6524, 5. rue Kessler, F-63 038 Clermont-Ferrand, France. (froger@opgc.univ-bpclermont.fr)

T. Souriot and Y. Fukushima, Laboratoire Magmas et Volcans, Université Blaise Pascal-UMR 6524, 5 rue Kessler, F-63 038 Clermont-Ferrand, France.

T. Staudacher, Observatoire Volcanologique du Piton de la Fournaise, Institut de Physique du Globe de Paris, 14 RN3, le 27ème, F-97418 La Plaine des Cafres, La Reunion.

N. Villeneuve, Centre de recherches et d'études en géographie de l'Université de La Réunion (CREGUR), Université de la Réunion, 15 avenue René Cassin, BP 7151 97715 Saint-Denis, Messag Cedex 9, La Reunion.